RC22860 (W0307-186) July 29, 2003
Materials Science

IBM Research Report

Finite Size Effects in Stress Analysis of Interconnect Structures

Ismail C. Noyan, Conal E. Murray, [1]Charles C. Goldsmith, S. Chey

IBM Research Division
Thomas J. Watson Research Center
P.O. Box 218
Yorktown Heights, NY 10598

[1]IBM Microelectronics Division,
Hopewell Junction, NY 12533

Research Division
Almaden - Austin - Beijing - Delhi - Haifa - India - T. J. Watson - Tokyo - Zurich

Finite Size Effects in Stress Analysis of Interconnect Structures

I. C. Noyan* and Conal E. Murray

IBM Research Division, T. J. Watson Research Center, Yorktown Heights, NY 10598

I.
Charles C. Goldsmith

IBM Microelectronics Division, Hopewell Junction, NY 12533

Jay S. Chey
IBM Research Division, T. J. Watson Research Center, Yorktown Heights, NY 10598

Abstract

Conventional formulations of thermal stress evolution in interconnect structures usually ignore the interfaces between the various levels. In this article we present thermal and residual stress versus temperature data from simple copper-thin-film structures on silicon. The results indicate that interconnection models which assume fully elastic behavior and ideal interfaces may yield inaccurate predictions of the thermo-mechanical response for feature sizes smaller than 10 micrometers.

* noyan@us.ibm.com

The topology of most integrated circuits in current production consists of patterned thin films of conductors and dielectrics stacked on thick semiconductor substrates containing active devices. From a strength-of-materials perspective such structures can be classified as heterogeneous composite systems. Analysis of the thermo-mechanical response of these systems is non-trivial. Analytical formulations are available only for the simplest geometries such as stacks of continuous thin films on a substrate[1-8]. For most multilevel interconnection nets with complex geometries, numerical solutions, such as those based on finite-element analysis, have been used[9,10]. Both analytical and numerical models contain many simplifying assumptions such as the use of linear elastic constitutive equations and constituents with isotropic symmetry. For systems undergoing cyclic thermal excursions, the mechanical constants of the composite are generally assumed to be invariant with the number of thermal cycles. Most models, with the exception of the shear-lag (S-L) model of Chen and Nelson[3], also ignore the integrity of the interfaces between the various layers. The S-L formulation explicitly assigns a shear modulus and thickness, G_i, t_i, to each interface and describes the stresses in each layer as a function of position from one end of the composite to the other. For the simplest case of a one-dimensional thin film feature with the cross-sectional geometry depicted in Figure 1, the local normal stress, σ_{xx}^{f}, produced in the feature of Young's modulus E_f and coefficient of thermal expansion α_f due to a temperature excursion ΔT from the zero-stress temperature possesses the form[11] :

$$\sigma_{xx}^{f} \sim E_f \Delta T (\alpha_f - \alpha_s) \left[\frac{\cosh(\beta x)}{\cosh(\beta l)} - 1 \right] \qquad \beta \propto \sqrt{\frac{G_i}{t_i}\left(\frac{1}{E_f t_f} + \frac{1}{E_s t_s}\right)} \quad (1).$$

where β represents the eigenvalue of the thin film / substrate system.

As described by Equation 1, the normal stress in the film tends to zero as one approaches the free edges. The rate of the decay is dictated by the eigenvalue β. Because β is a function of the material parameters of the thin film, substrate and interfacial layer, the decay rate is independent of the feature size. It becomes useful to define a critical feature size at which the normal stress in the film reaches a predetermined fraction (for example 95%) of the stress in an infinitely long feature. Using Equation (1), the critical length, $\mathbf{l_c}$, can be represented as:

$$l_c = 2\frac{\cosh^{-1}(20)}{\beta} \quad (2).$$

For features with lengths less than $\mathbf{l_c}$, the edge effects begin to dominate the overall stress distribution whereas features larger than $\mathbf{l_c}$ contain a central region with stress values greater than 95% of the stress in an infinite feature.

The average stress within the feature can be obtained by integrating Equation 1 over the feature size. For an infinitely long feature, the volume fraction of the regions affected by the free edges is negligible, and the average stress approaches the Timoshenko limit[1,2,8] :

$$\sigma_{xx}^{f} \cong \frac{\Delta T(\alpha_f - \alpha_s)}{t_f\left(\frac{1}{E_f t_f} + \frac{1}{E_s t_s} + \frac{3\left(t_f + t_s\right)^2}{E_f t_f^3 + E_s t_s^3}\right)} \quad (3).$$

On the other hand, if the size of the feature is reduced, the average stress drops below the Timoshenko limit as **l** approaches $\mathbf{l_c}$ and tends to zero in the limit of an infinitesimal feature. By monitoring the average stress in samples of various sizes as a function of temperature, one should be able to obtain information about the critical length, and consequently, the interface parameters between a thin film and its substrate through the use of Equations 1 to 3. In the following, we describe the results of such a study.

The samples used in this study consisted of patterned and blanket Cu thin films evaporated on an adhesion layer of 100 A thick Cr on Si (001) wafers 5" in diameter. Pattern dimensions and manufacturing conditions are given in Table I, and typical sample geometry is shown in Figure 2. To aid comparisons, blanket and patterned films were obtained from different regions of the same wafer for both cases.

The diffraction measurements were carried out on a Rigaku RINT 2100 –Ultima theta-theta diffractometer equipped with a controlled-atmosphere, high-temperature heating stage. For stress measurements, the standard x-ray $\sin^2\psi$ method was used with Cu 311 and 222 reflections and Fe Kα radiation. The nominal irradiated area on the sample at symmetric incidence (ψ =0) was 10 x15 mm^2. Since many dots contributed to the

diffraction signal (Table I), the measured stresses are average values. All measurements were conducted in a forming-gas atmosphere.

Variation of the average thermal stresses with temperature in Sample Set 1 is shown in Figure 3. The results from the blanket region agree with those reported in the literature for the first temperature cycle of an evaporated Cu thin film[12]; initially the Cu film exhibits tensile deposition stresses. As the film is heated, the difference between the thermal expansion coefficients of Cu and Si (~14 10^{-6} /^{o}C) causes the formation of compressive thermal stresses in the film, and the total stress decreases with temperature. Between room temperature and 100 ^{o}C, the stress variation agrees quite well with the Timoshenko formulation (dashed line in Figure 3). Above this temperature, plasticity and subsequently creep effects dominate the mechanical behavior of the composite: elastic analysis does not apply. During cooling, tensile residual stresses are generated due to the CTE mismatch and the final residual stress is highly tensile. The temperature profile during these measurements was step-wise continuous. For each data point, the stress measurement was carried out at constant temperature (~30 minutes per measurement), and then the sample was ramped to the next measurement temperature.

The stress-temperature response of the 3 μm dot region from the same wafer and subjected to the same temperature cycle is significantly different. Lower average film stresses are measured for the patterned region at all temperatures and the Timoshenko formulation is not applicable anywhere.

To quantify the differences between the blanket and patterned thin film response, we measured the average retained thermal residual stress (RTRS) at room temperature after each annealing step. Thus, the temperature profile is of the form 25 ^{o}C, 50 ^{o}C, 25 ^{o}C, 100 ^{o}C, 25 ^{o}C, 150 ^{o}C, 25 ^{o}C, etc. The stress state at room temperature is in static equilibrium and the measurements yield only residual stresses. The RTRS results for the 3 μm and 14 μm patterned samples are shown in Figures 4-a, b. It can be seen that the retained residual stresses within the 14 μm features are equivalent to the blanket film stresses over the entire range. Thus, 14 μm features are at the continuum limit and can be treated by equations derived for blanket films. On the other hand, in agreement with the continuous heating/cooling curves shown in Figure 3-b, the RTRS values of the 3 μm features are lower than the values measured from the blanket film. Thus, finite-size formulations are needed to model the thermo-mechanical response for such feature sizes for this system.

It is possible to obtain quantitative interface parameters from the data shown in Figures 4-a,b. Let us define the stress ratio, ***SR***, as the ratio of the retained thermal residual stress in the patterned features to that of the equivalent blanket film. Based on the data in Figure 4-a, the stress transfer coefficient of the 14 μm features is approximately unity for all temperatures. The variation of ***SR*** values with temperature for the 3 μm features is shown in Figure 5. It is seen that ***SR*** values reach a maximum of approximately 0.45 after the highest temperature anneal. We note that subsequent thermal cycles to this temperature did not change this value. An examination of Equation 1, which describes the stress in an elastically isotropic film reveals that the interfacial compliance ratio G_i/t_i is the only

parameter that would change with temperature. By integrating Equation 1 over the feature length and using the average stress measured by x-ray diffraction, we can calculate G_i/t_i. For the stress values shown in Figure 4-b, this parameter changes from 28.5 GPa/μm to 285 GPa/μm. It appears that during the first temperature cycle the interface evolves and becomes "stronger". If we assume an unchanging interface thickness of 1nm, this indicates that the shear modulus of the interface changes from 28.5 MPa to 285 MPa with repeated heating and cooling. Alternatively, if we assume that the shear modulus of the interface is invariant, say at 285 MPa, the interface thickness must change from 10 nm to 1 nm. It is possible that both mechanisms contribute to the observed variation. We note that this variation is not due to microstructural changes and is under further study[13] .

Using the experimentally determined interfacial stiffness ratio, G_i/t_i, one can calculate the local variation of film stress with position in the features. These values are plotted in figures 6-a,b for the 3 and 14 μm features, respectively. The average stress for the 14 μm feature based on the profile shown in Figure 6-b is 88% of the Timoshenko limit. This value matches the experimentally measured average stresses shown in Figure 4-a. Consequently, the interface parameters of both sample sets appear to be equivalent. We must note that, for the 14 μm pattern, the invariance of the ***SR*** values with temperature cycling does not necessarily mean an invariant interface. Since the sample size is significantly greater than the critical length, any strengthening of the interface would not be reflected in the measured average stress values and consequently the ***SR*** values.

In conclusion, it appears that interface parameters play an important role in the thermo-mechanical response of interconnect structures with small sizes. These interface parameters cannot be assumed to be constant with processing. Models that do not explicitly specify these interface parameters cannot predict the thermo-mechanical response of even the simplest structures and should be used with due caution. Formulations that consider the film or substrate to be infinite, such as the Timoshenko equation, should not be used for the analysis of thermal stress data from samples with sizes comparable to the shear-lag critical length. In the case of the Cu features characterized in this study, the average stress determined will deviate significantly from the Timoshenko limit for features smaller than 10 μm. This size is dependent on the interfacial stiffness ratio, G_i/t_i, and must be determined experimentally for other systems.

References

(1) S. Timoshenko, *J. Opt. Soc. Amer*., {11}, 233 (1925).

(2) S. Timoshenko, and S. Woinowsky-Krieger, *Theory of Plates and Shells, 2nd Ed*., McGraw-Hill, New York, 1959

(3) I.A. Blech, and E.S. Meieran, *J. Appl. Phys*., {38}, 2913 (1967).

(4) W.T. Chen, and C.W. Nelson, *IBM J. Res. Develop*., {23}, 179 (1979).

(5) E. Suhir, *J. Appl. Mech*., {53}, 657 (1986).

(6) E. Suhir, *J. Appl. Mech*., {56}, 595 (1989).

(7) C-H Hsueh, J. Appl. Phys.(92), 144 (2002)

(8) C. E. Murray, I. C. Noyan , *Phil. Mag. A*, (2002).

(9) M.S. Kilijanski,. Y. L. Shen, *Microelectron. Reliab*. (42), 259 (2002).

(10) S-H. Rhee, Y. Du, P. S. Ho, Journal of Applied Physics (93) 3926 (2003).

(11) The expressions in Equation 1 to 3 are used to illustrate the general dependence of the normal stress on the material properties and geometry. In the application of the S-L model to the experimental stress measurements, we use a two-dimensional solution that incorporates the effects of bending within the thin film and substrate system. Details of this formulation can be found in Murray and Noyan [7].

(12)M. D. Thouless, K. P. Rodbell, C. Cabral, Jr., J. Vac. Sci. tech. A, (14) 2454, 1996.

(13) Integrated intensity measurements of the first five Cu reflections during thermal cycling showed that microstructural evolution in both blanket and patterned films were identical.

Sample ID	Film Type	Thickness	Nominal Pattern Dimensions	# of dots in x-ray beam	Pattern Process
Set 1	Blanket + pattern	~1μm	14x14 μm squares on 40 μm centers.	~10^5	Evaporation through a mask
Set 2	"	~1μm	3x3 μm squares on 5 μm centers	.~$6x10^6$	Pattern and etch

Table I: Sample geometries used in the study. Both sets were evaporated at nominally room temperature. The blanket regions were obtained from 30 mm-wide annular regions near the wafer edges.

Figure Captions

Figure 1: Typical sample geometry for the shear-lag model. For evaporated films, the interface region is not well-defined. One can define this region as the volume where neither the film nor the substrate symmetry operators are fully applicable.

Figure 2: Representative FIB images of the pattern area from Sample Set 2. The Cu features are nominally 3 μm long and wide, on 5 μm centers. The etching removed a shallow annulus of Si around each feature. TEM cross-sections did not reveal any interface damage.

Figure 3: Average stress variation with temperature for the pattern and blanket regions of Sample Set 2. The dashed line indicates the stresses obtained from Equation (3).

Figure 4-a: Variation of average retained thermal residual stress values at room temperature with annealing temperature for Sample Set 1. The stress values from the patterned region are equal to those determined from the blanket region.

Figure 4-b: Variation of average retained thermal residual stress values at room temperature with annealing temperature for Sample Set 2. The stress values from the patterned region are much lower from those determined from the blanket region.

Figure 5: Variation of the stress ratio, ***SR***, with temperature for Sample Set 2 (3 μm features). The ***SR*** values reach a maximum of ~0.45 after the highest temperature anneal of the first cycle and do not change with subsequent cycles.

Figure 6-a: Variation of the local stress $\sigma_{xx}^{f}(x)$ with position in a 3 μm feature (6-a), and in a 14 μm feature (6-b) calculated from Equation (1) using the interfacial stiffness ratio, G_i/t_i, determined from Figure 4-a. The average stress in Figure 6-b matches the experimentally measured values in Figure 4-b, indicating that the interfaces of Sample sets 1 and 2 are equivalent.

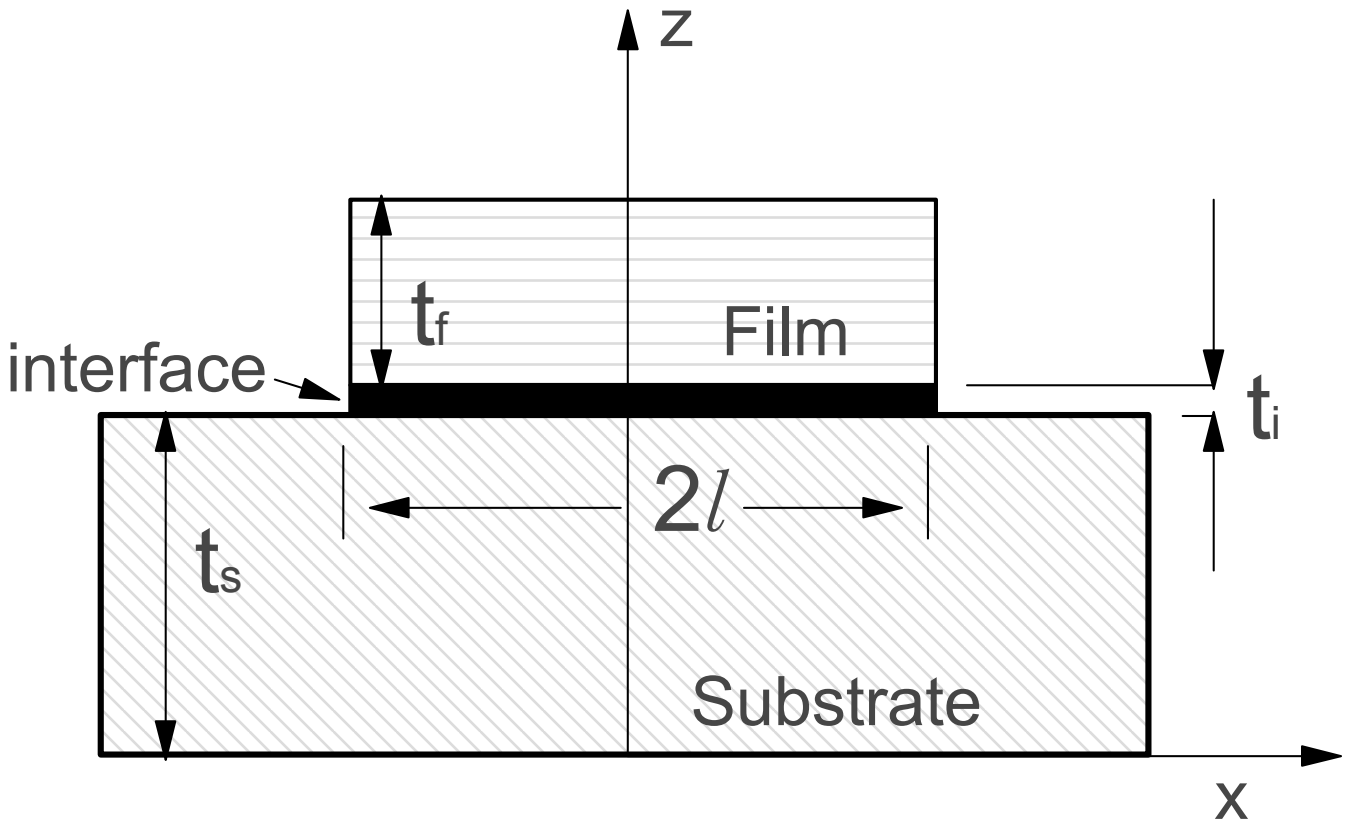

Figure 1

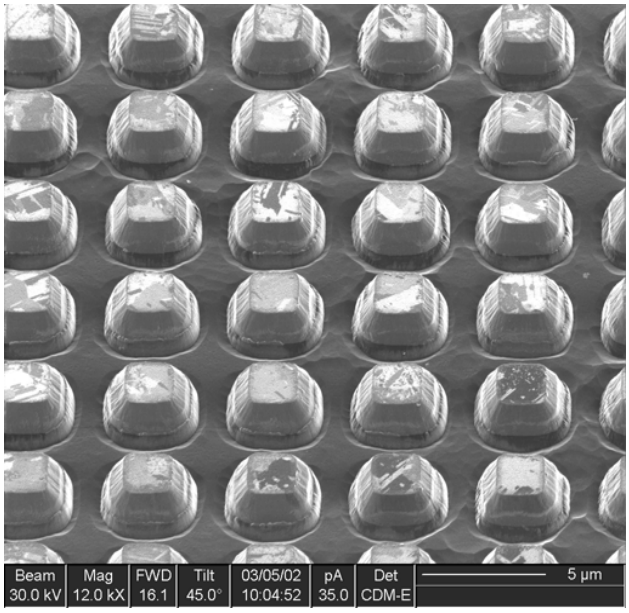
Beam
30.0 kV
Mag
12.0 kX
FWD
16.1
Tilt
45.0°
03/05/02
10:04:52
pA
35.0
Det
CDM-E
5 µm

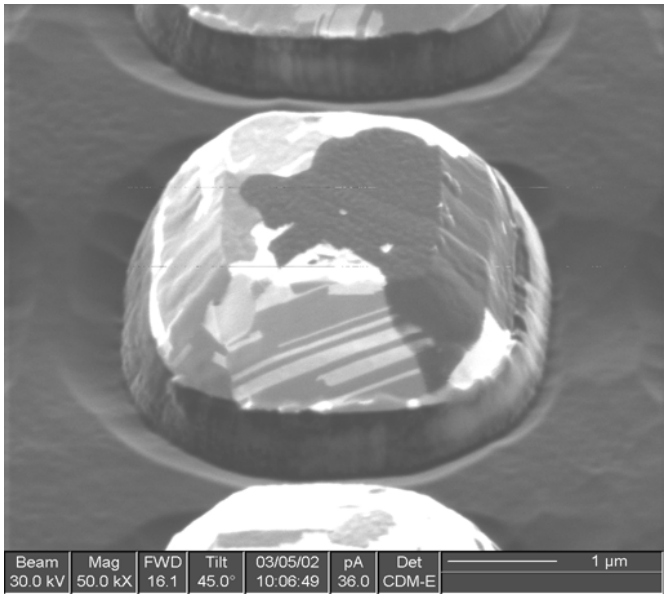
Beam
30.0 kV
Mag
50.0 kX
FWD
16.1
Tilt
45.0°
03/05/02
10:06:49
pA
36.0
Det
CDM-E
1 µm

Figure 2

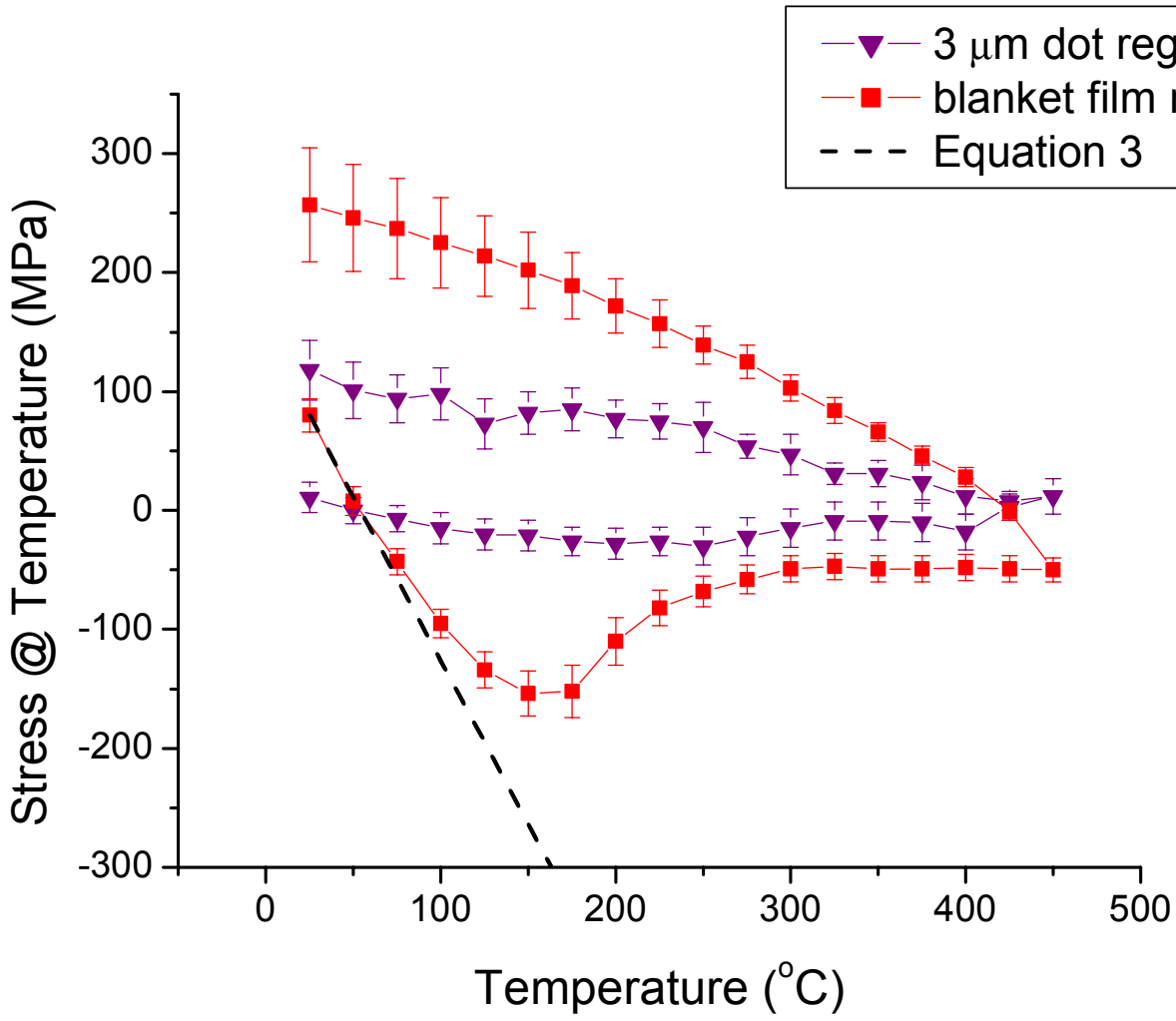
3 μm dot region
blanket film region
Equation 3
Stress @ Temperature (MPa)
300
200
100
0
-100
-200
-300
0
100
200
300
400
500
Temperature (°C)

Figure 3

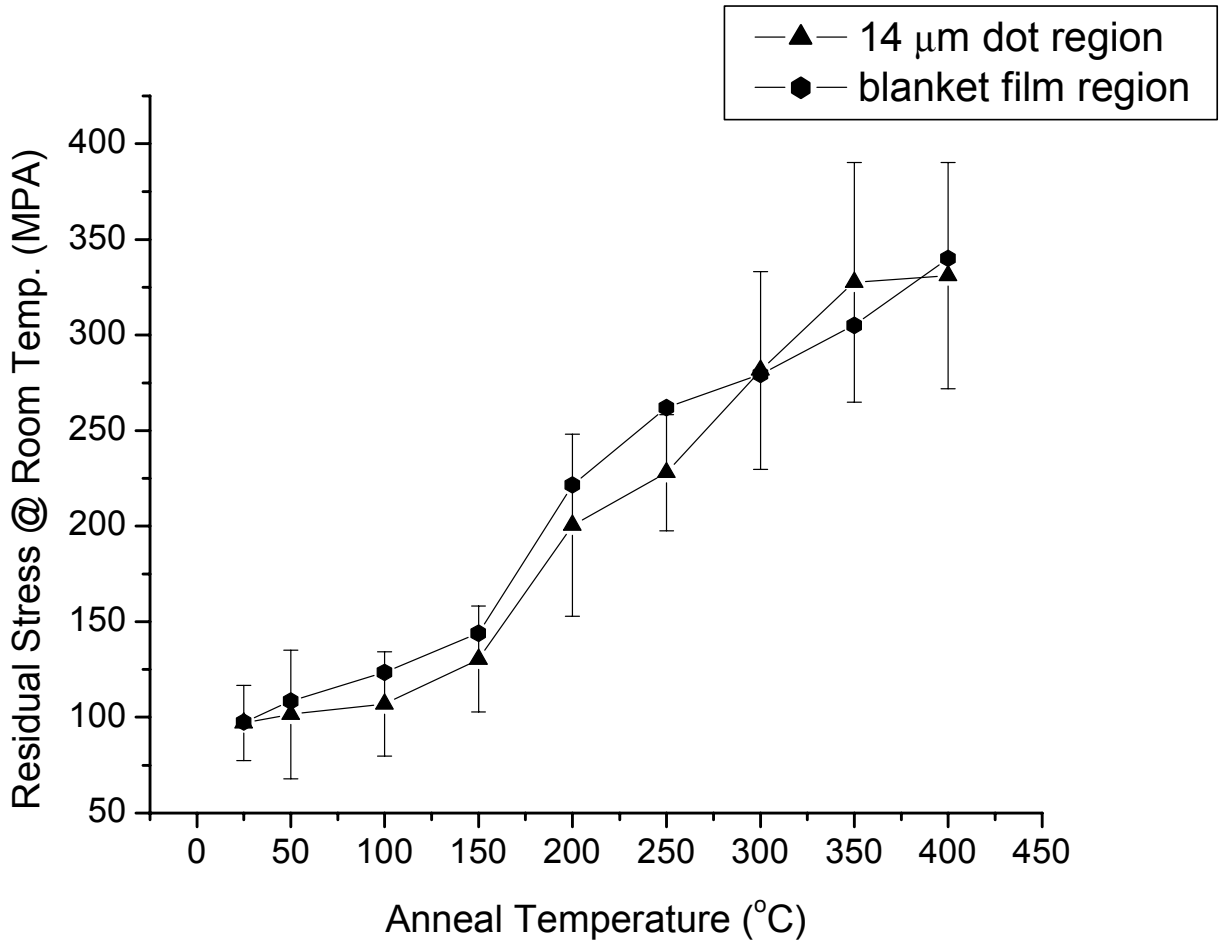
14 μm dot region
blanket film region
Residual Stress @ Room Temp. (MPA)
400
350
300
250
200
150
100
50
0
50
100
150
200
250
300
350
400
450
Anneal Temperature (°C)

Figure 4-a

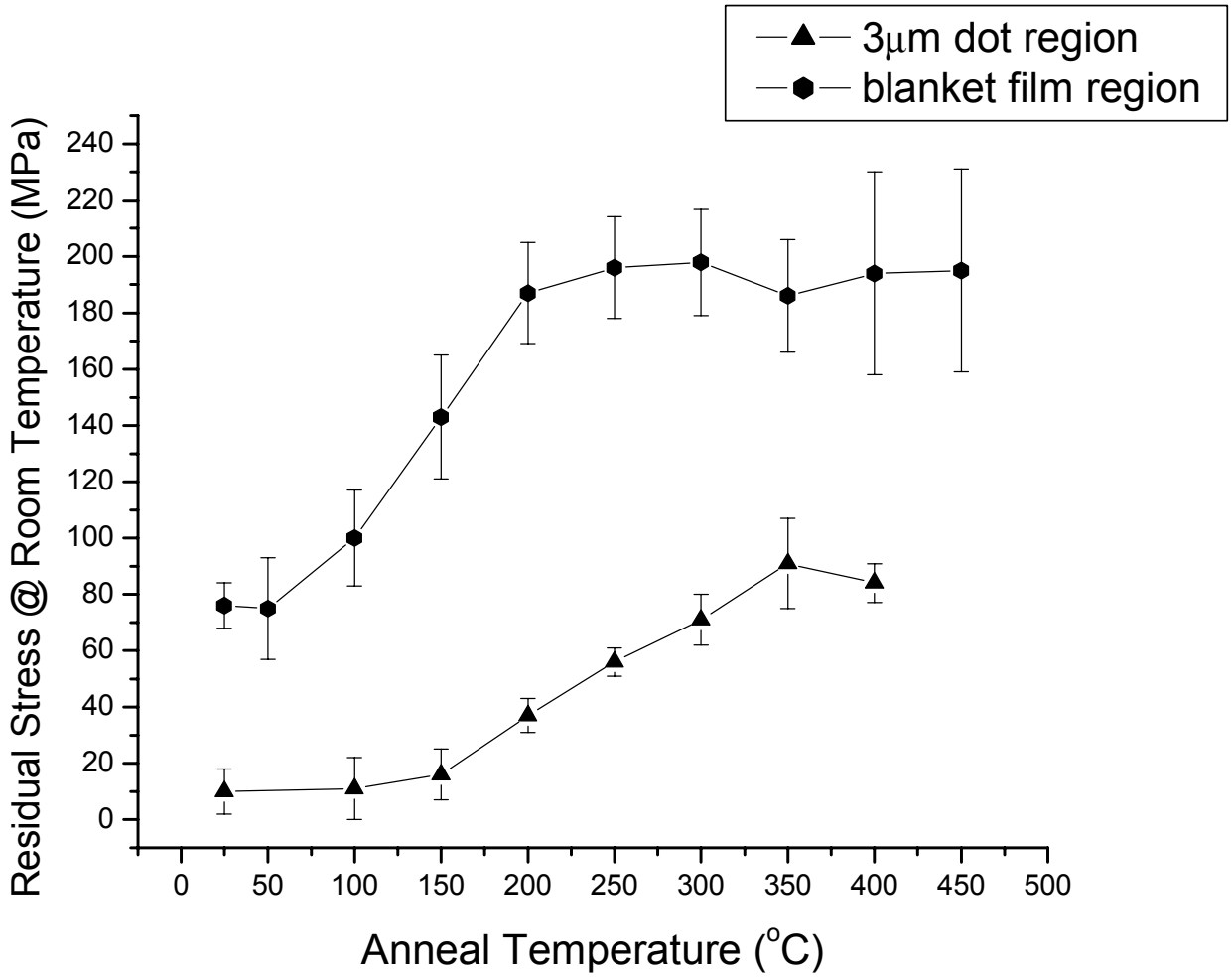
3μm dot region
blanket film region
Residual Stress @ Room Temperature (MPa)
0
20
40
60
80
100
120
140
160
180
200
220
240
0
50
100
150
200
250
300
350
400
450
500
Anneal Temperature (°C)

Figure 4-b

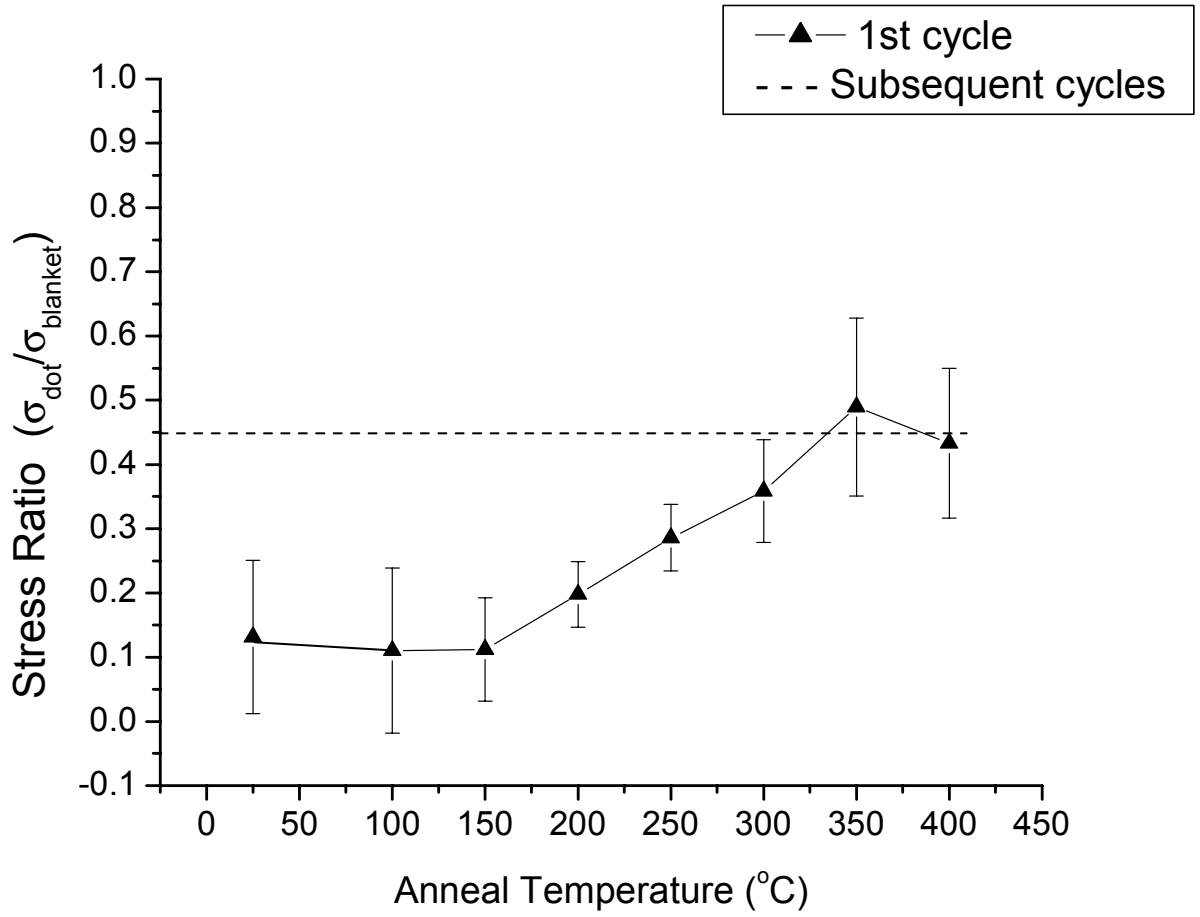
1st cycle
Subsequent cycles
Stress Ratio ($\sigma_{dot}/\sigma_{blanket}$)
1.0
0.9
0.8
0.7
0.6
0.5
0.4
0.3
0.2
0.1
0.0
-0.1
0
50
100
150
200
250
300
350
400
450
Anneal Temperature (^{o}C)

Figure 5

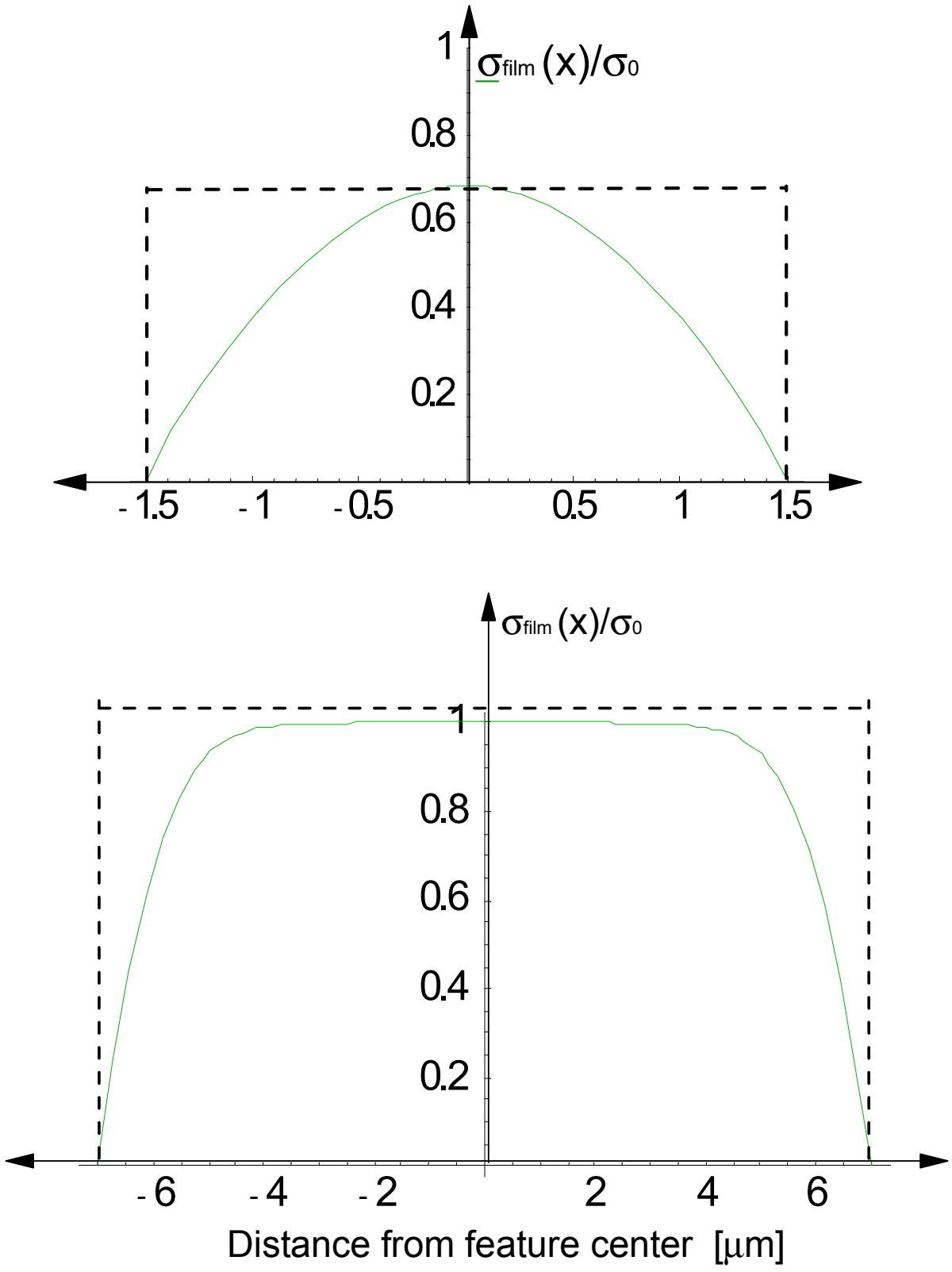
σfilm (x)/σ0
1
0.8
0.6
0.4
0.2
-1.5
-1
-0.5
0.5
1
1.5
σfilm (x)/σ0
1
0.8
0.6
0.4
0.2
-6
-4
-2
2
4
6
Distance from feature center [μm]

Figure 6 a,b